ACS OMEGA

http://pubs.acs.org/journal/acsodf

Article

Experimental and Kinetic Studies of Ethylene Glycol Autoignition at High Temperatures

Ping Xu, Rui Wang, Tao Ding, Weixin Tang, and Changhua Zhang*

Cite This: *ACS Omega* 2022, 7, 9044−9052

Read Online

ACCESS | Metrics & More | Article Recommendations | Supporting Information

ABSTRACT: As one of the simplest polyols with chemical properties of alcohol, ethylene glycol is considered as a renewable energy source and a model fuel for pyrolysis oil. In this work, autoignition characteristics of ethylene glycol have been investigated behind reflected shock waves. Experiments were conducted at pressures of 2, 5, and 10 atm, equivalence ratios of 0.5, 1.0, and 2.0, and temperatures ranging from approximately 1200 to 1600 K. The fuel concentration was also varied. Results show that the ignition delay time increases with decreasing the pressure or fuel concentration. A strong positive dependence upon the equivalence ratio was found. A quantitative relationship has been yielded by the regression analysis of the experimental data. Simulations were carried out using chemical kinetic mechanisms available in the literature to assess the reliability of mechanism. Reaction pathway and sensitivity analysis confirmed the importance of H-abstraction reactions in ethylene glycol oxidation process. Finally, a comparison between ethylene glycol and ethanol ignition was conducted. Ethylene glycol ignites faster than ethanol because of the early accumulation of H and OH radicals in the oxidation of ethylene glycol.

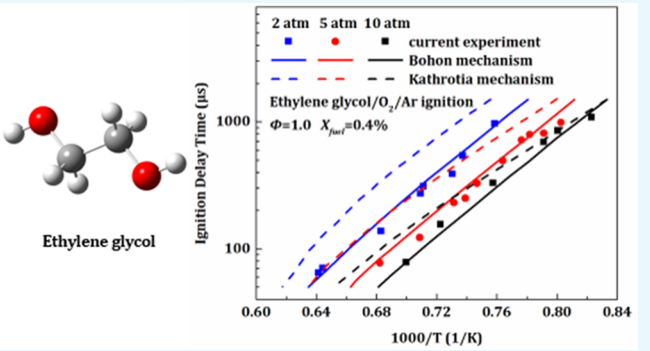

1. INTRODUCTION

Diesel engines are used worldwide for transportation and power generation due to their high thermal efficiency, reliability, and durability.[1−5] However, various global environmental issues related to fossil fuels are becoming more serious. It is well-known that adding oxygenated fuels to diesel fuel can effectively reduce the particulate matter (PM) and NOx emissions of compression ignition engines.[6−12] As an alternative renewable source, alcohols are considered as one of the most promising additives for fossil fuels. Until now, a large amount of efforts has been carried out to investigate the effect of alcohols on the performance, exhaust emissions, and combustion characteristics of fossil fuels under diesel engine conditions, especially for low carbon number monohydric alcohols, namely methanol up to butanol.[13−19] Owing to the hydroxyl functional group in the alcohol molecule, the oxidation of the fossil fuels can be more efficient and cleaner, and less PM are formed.

Polyol is a group of compounds with multiple hydroxyl functional groups. Ethylene glycol (EG) is an important representative in polyols, which contains two hydroxyl groups attached to the ethane molecule. The chemical formula is $OH-CH_2-CH_2-OH$ and has a high content of oxygen (51.6 wt %). It is observed that EG has similar oxidation reactivity and ignition characteristics as ethanol, indicating that EG has the potential for use as a supplement for ethanol.[20,21] The emissions of nitrogen oxides and soot can be reduced when EG in blended in diesel.[22−24] Moreover, EG is often selected as a single-component surrogate for the pyrolysis oil, which is a bio-oil used as a substitute for fossil fuels in turbines and internal combustion engines, because that EG has similar chemical and physical properties to those of pyrolysis oil.[25−28] In order to model the pyrolysis and combustion processes of EG in practical systems, it is necessary to investigate the reaction kinetics of EG and construct the combustion kinetic mechanism that has been assessed against fundamental experimental data. On the basis of the literature survey, only a few studies have been focused on the kinetic of EG combustion. Ye et al.[29] have theoretically studied the unimolecular decomposition of EG, and they found that the H_2O elimination reactions are predominant at a low temperature of 500−1075 K and the direct C−C bond dissociation reactions are dominant at a high temperature of 1075−2000 K. Li et al.[30] have calculated the anharmonic effect on the dissociation of EG and the result of EG decomposition was similar to that of Ye et al.[29] Based on the kinetics model of

Received: January 13, 2022
Accepted: February 24, 2022
Published: March 4, 2022

https://doi.org/10.1021/acsomega.2c00275
ACS Omega 2022, 7, 9044−9052

Hafner et al.,[31] a detailed oxidation mechanism for EG has been developed by Kathrotia et al. which consists of 78 species and 574 reactions.[32] Further reduced and global mechanisms derived from the mechanism of Kathrotia et al. have been used for computational fluid dynamics (CFD) simulations of the entrained flow gasification.[25,27,28,33] Bohon et al.[34] have investigated the influence of molecular structure in hydroxylated fuels on NOx formation. These experiments show significantly lower NOx formation with increasing fuel oxygen content despite similarities in the flame temperature profiles. A detailed high temperature chemical kinetic mechanism has been developed based on the previous alcohol combustion mechanism and extended to include EG combustion chemistry, which consists of 482 species and 2809 reactions. Ignition delay time is one of the key sources of data that is important to characterizing the combustion properties of real fuels and has been extensive used in the development and assessment of combustion reaction mechanisms. However, very limited studies were performed on the autoignition of EG except that Kathrotia et al. have measured the ignition delay times of EG in air in a temperature range of 800−1500 K at a pressure of 16 bar.[32] The ignition data of EG are still lacking, and a systematic investigation on EG ignition covering a wide range of experimental conditions is necessary.

In this study, the ignition delay times (τ) of EG diluted in argon were measured behind reflected shock waves at pressures (P) of 2, 5, and 10 atm, equivalence ratios (Φ) of 0.5, 1.0, and 2.0, fuel concentrations (X) of 0.4% and 0.2%, and temperatures (T) ranging from approximately 1200 to 1600 K. Two chemical kinetic mechanisms (Kathrotia et al.[32] and Bohon et al.[34]) were assessed by comparing the measured and calculated ignition delay times. Further insight into the EG oxidation kinetics has been discussed in detail.

2. EXPERIMENTAL SECTION

Ignition delay time measurement was conducted in a heated stainless steel shock tube with an inner diameter of 10 cm, which is divided into a 2 m driver section and a 5 m driven section separated by a double diaphragm section. The driven section can be heated with an electronically controlled heating system to ensure that the test mixtures is always in gas phase. High-purity helium (99.999%) was used as the driver gas. Nine independent current circuits were used to provide a uniform temperature distribution along the tube length with uncertainty of less than 3 K at 120 °C.[35] Polyester terephthalate (PET) diaphragms with different thicknesses were chosen to obtain different reflected shock pressures. The shock tube was evacuated below 1.0 Pa using a vacuum system before each experiment. Further detailed description on the shock tube can be found in previous publications.[36,37]

Fuel mixtures of EG (99% purity), oxygen (99.999% purity) and argon (99.999% purity) were prepared manometrically in a heated mixing tank. To ensure that the test mixture in gas phase, the gas tank was heated and kept to 423 K. Moreover, the mixture was allowed to sit for at least 2 h to guarantee fully mixed before the first ignition experiment. The detail compositions of experimental mixtures are listed in Table 1.

Four fast-response pressure transducers on the sidewall (PCB 113B) were used to measure the velocity of the incident shock wave, which was used to calculate the temperature and pressure of the mixtures behind the reflected shock waves by the one-dimension normal-shock model of Chemkin-Pro software.[38] In addition, light emission during ignition was detected by a quartz optical fiber, which was installed at the same cross section of the last pressure transducers located 15 mm away from the endwall of the shock tube. The fiber was then fed into a grating monochromator coupled with a photomultiplier to collected the CH* chemiluminescence at 431 nm.

Table 1. Detailed Compositions of the Experimental Mixtures

mixture	Φ	EG (%)	O_2 (%)	Ar (%)
1	0.5	0.4	2.0	97.60
2	1.0	0.4	1.0	98.60
3	2.0	0.4	0.5	99.10
4	1.0	0.2	0.5	99.30
5	1.0	1.5	3.75	94.75

In current work, the ignition delay time was defined as the time interval between the arrival of the shock wave detected by the last pressure transducer at the sidewall (defining time zero) and the time of extrapolating the maximum slope of CH* emission signal back to the baseline. An example of ignition delay time measurement is provided in Figure 1. The overall deviation of measured ignition delay time in this work is estimated to be within ±20%.[37]

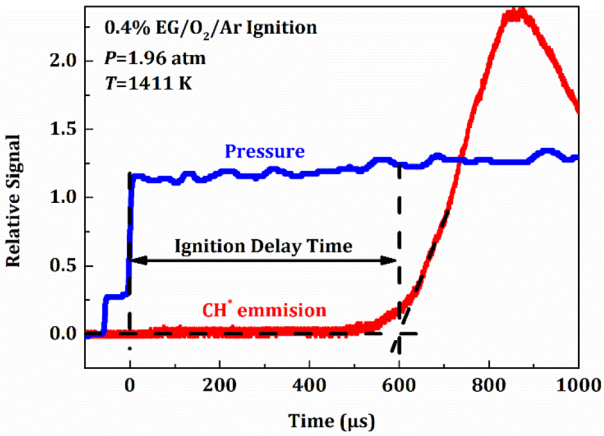

Figure 1. Representative pressure and CH* emission histories. The definition of the ignition delay time is also indicated.

3. RESULTS AND DISCUSSION

3.1. Ignition Delay Times. Ignition delay times of EG/O_2/Ar mixtures were measured at the temperatures ranging from 1200 to 1600 K, pressures of approximately 2, 5, and 10 atm, and equivalence ratios of 0.5, 1.0, and 2.0 with different fuel concentrations. The ignition delay times measured during this study are summarized in the Supporting Information. The ignition delay time at high temperature shows the Arrhenius dependence upon the temperature. Therefore, an Arrhenius-based, power law expression has been used to correlate the ignition delay time in combination using Arrhenius temperature dependence and power-law dependence on equivalence ratio, pressure and fuel concentration. This correlation form has been used successfully in many previous studies for hydrocarbons and alcohols.[39,40] A regression analysis of the experimental data yields the following correlation with r^2 = 0.972 for EG/O_2/Ar ignition delay times:

https://doi.org/10.1021/acsomega.2c00275
ACS Omega 2022, 7, 9044−9052

$$\tau = (2.32 \pm 0.25) \times 10^{-5}\Phi^{(0.94\pm0.03)}P^{-(0.57\pm0.02)} X_{EG}{}^{-(0.33\pm0.06)} \exp[(42.02 \pm 0.73)/RT]$$

Here τ is the ignition delay time in microsecond, Φ is the equivalence ratio, P is the ignition pressure in atmospheric pressure, X_{EG} is the initial mole fraction of EG in the mixtures, T is the ignition temperature in Kelvin and R is the universal gas constant in cal·mol^{-1}·K^{-1}. In the following ignition figures, small pressure variations from the common pressure have been scaled in advance using the power law relationship $\tau \sim P^{-0.57}$. All ignition delay times have been scaled to a common condition using the determined power-law dependence, as shown in Figure 2. It can be seen that the plot is quite linear

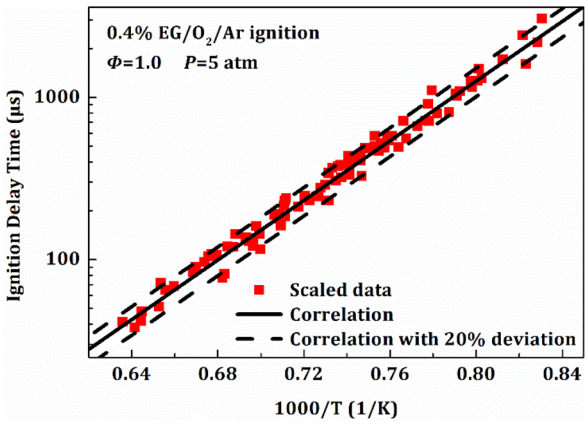

Figure 2. Ignition delay times scaled to a common condition of Φ = 1.0, P = 5 atm, and X_{EG} = 0.4% using the correlation with 20% deviation.

with a slope that equates to an activation energy of 42.02 ± 0.73 kcal/mol, and ±20% shifts of the correlation line have been given. Figure 2 shows the scattering of the experimental data around the correlation curve within the deviation of 20%. Thus, in the following experimental ignition figures, a ±20% ignition delay time deviation bar has been given.

The effect of pressure on ignition delay times was studied at three equivalence ratios (0.5, 1.0, and 2.0) and two fuel concentrations (0.2% and 0.4%). Figure 3 displays the effect of pressure on the ignition delay time of EG/O_2/Ar mixtures at 2, 5, and 10 atm. The ignition delay time exhibits a systematic decrease with increasing pressure, in other words, the reactivity increases with the pressure for a given equivalence ratio. The same trend is observed at different equivalence ratios and fuel concentrations in Figure 3, which indicates a consistent trend of reactivity of EG oxidation with pressure for all conditions studied in this work.

The effect of equivalence ratio on ignition delay times of EG/O_2/Ar mixtures was determined by measuring ignition delay times for 0.4% fuel concertation at 2, 5, and 10 atm. The oxygen concentration was altered by fixing the fuel concentration to obtain various equivalence ratios in this work. Figure 4 shows the effect with equivalence ratios of 0.5, 1.0, and 2.0.

As can be seen, the dependence of ignition delay times shows the same trend at 2, 5, and 10 atm that increasing the equivalence ratio from 0.5 to 2.0 results in an increasing ignition delay time. That is, the fuel-lean mixture (Φ = 0.5) is the most reactive, whereas the fuel-rich mixture (Φ = 2.0) is the least reactive. It is well-known that the chain-branching reaction H + O_2 = O + OH has a strong promoting effect on fuel ignition at high temperatures, which can be obtained from the sensitivity analysis later. In Figure 4, the mole fraction of EG was kept at 0.4%, and the oxygen concentration was varied from 2.0% to 0.5% when the equivalence ratio increases from 0.5 to 2.0. Therefore, from fuel-lean to fuel-rich conditions, the chain-branching reaction was weakened, and as a result, a decline in reactivity can be observed from fuel-lean to fuel-rich conditions, leading to the positive dependence of equivalence ratio on ignition delay time.

The effects of fuel concentration on ignition delay time of EG at an equivalence ratio of 1.0 are displayed in Figure 5. As expected, the ignition delay time of higher fuel concentration is shorter than that of lower fuel concentration at pressures of 2, 5, and 10 atm, respectively. A negative dependence on dilution ratio is obtained.

3.2. Mechanism Comparison. The simulation of ignition delay times was performed with a zero-dimensional closed homogeneous reactor in the Chemkin-Pro package.[38] Constant volume and adiabatic assumptions (CONV) were carried out. The simulated ignition delay times are defined in line with the diagnostic method of shock-tube measurement. Two available mechanisms from Kathrotia et al.[32] and Bohon et al.[34] were used. Assessment of kinetic mechanisms of EG was carried out by comparison of mechanism simulations with current experimental measurements. Figures 3−5 also show the comparison. Overall, predictions of these two mechanisms are found to be in qualitative agreement with the experimental results. Both mechanisms can well predict the effects of temperature, pressure, equivalence ratio, and fuel concertation. The Bohon mechanism gives good quantitative agreement with the experimental data at different pressures and equivalence ratios, while the Kathrotia mechanism overpredicts the ignition delay times of EG/O_2/Ar mixtures significantly at most conditions. Thus, the mechanism of Bohon et al. was used for further kinetic analysis.

3.3. Chemical Kinetic Analysis. Chemical kinetic analyses have also been conducted to identify the important reaction pathways controlling EG autoignition using the mechanism of Bohon et al.[34] The reaction pathway analysis of stoichiometric EG was performed at a pressure of 5 atm, a temperature of 1350 K, and 20% fuel consumption. The result is shown in Figure 6. The consumption of EG is dominated by the H-abstraction reactions of H and OH radicals to produce $CH_2OHCHOH$ radical and a small portion to the CH_2OHCH_2O radical. Only 6.6% and 5.5% EG is consumed by H_2O elimination and C−C bond dissociation reactions, respectively. Both $CH_2OHCHOH$ and CH_2OHCH_2O radicals can undergo dehydrogenation reaction to produce the glycolaldehyde molecule (CH_2OHCHO), which will further react via H-abstraction followed by C−C dissociation reaction channel to form the hydroxymethyl radical (CH_2OH). A noticeable portion of the $CH_2OHCHOH$ radical can be consumed via the dihydroxylation reaction to produce the ethenol molecule (25.1%) or the dehydrogenation reaction to form a C−C double bonded diol (16.7%).

The rate of consumption analysis of EG has been performed at a typical condition of T = 1350 K, P = 5 atm, and Φ = 1.0 to further reveal important reactions of EG consumption, and the result is shown in Figure 7. The simulated ignition delay time using the mechanism of Bohon et al. under the typical conditions is 316 μs; however, the consumption of EG is conducted before the ignition event. Obviously, EG is

https://doi.org/10.1021/acsomega.2c00275
ACS Omega 2022, 7, 9044−9052

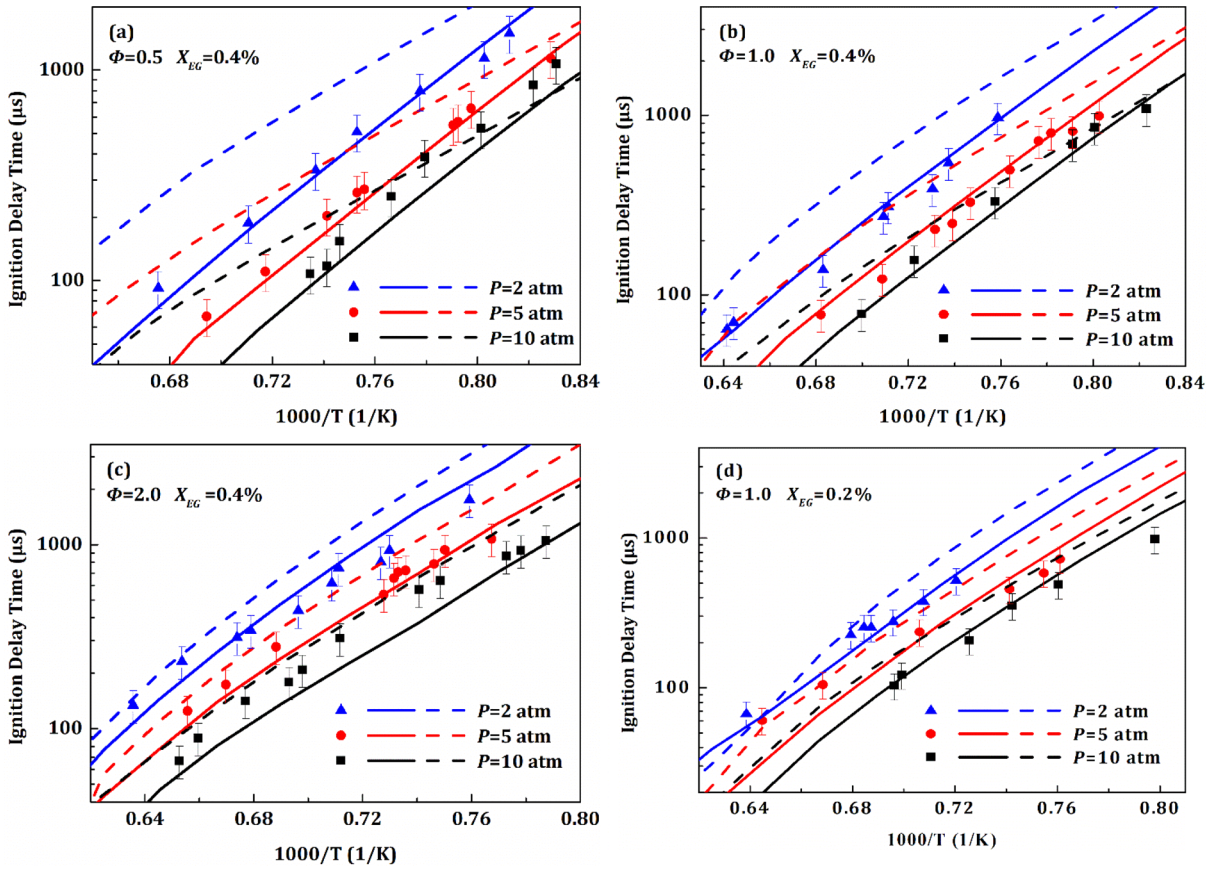

Figure 3. Effect of pressure on the ignition delay time of EG/O_2/Ar mixtures at (a) Φ = 0.5, X_{EG} = 0.4%; (b) Φ = 1.0, X_{EG} = 0.4%; (c) Φ = 2.0, X_{EG} = 0.4%; and (d) Φ = 1.0, X_{EG} = 0.2%, and a comparison with kinetic mechanisms. Symbols: Current experimental data. Solid line: Simulation results from the Bohon mechanism. Dashed line: Simulation results from the Kathrotia mechanism.

consumed predominantly via the C−C bond dissociation reaction to form the CH_2OH radical or via a H_2O elimination reaction to generate the C_2H_3OH molecule at the very beginning of the ignition process. H-abstraction reactions of H and OH dominate the consumption of EG to form the $CH_2OHCHOH$ radical after several microseconds. A much smaller proportion of EG is consumed via the formation of the CH_2OHCH_2O radical, which is in accordance with the pathway analysis of Figure 6.

Besides parent fuel and offspring related reactions, reactions involving H and OH radicals play an important role on fuel consumption, as shown in Figures 6 and 7. The rate of production (ROP) analysis for H and OH radicals are shown in Figure 8. At the initial stage, the dehydrogenation and dihydroxylation reactions from $CH_2OHCHOH$ radical are the key reactions for H and OH formation. The H-abstraction of fuel: EG + H = $CH_2OHCHOH$ + H_2 is the main consumption channel of H, and EG + OH = $CH_2OHCHOH$ + H_2O is the OH predominant consumption reaction. At the ignition time, H and OH are converted with each other by OH + H_2 = H + H_2O and H + O_2 = O + OH. O + H_2 = H + OH contributes to the formation of H and OH significantly.

In order to further study the specific reactions that are relevant to EG ignition in detail, a brute-force sensitivity analysis for ignition delay time has been performed using the chemical kinetic mechanism of Bohon et al.[34] by multiplying the rate constant of each individual reaction by two and calculating the change in the ignition delay time. The sensitivity coefficient is defined as $S = [\tau(2k_i) - \tau(k_i)]/\tau(k_i)$. Here, τ is the ignition delay time, and k_i is the reaction rate coefficient of the ith reaction. A negative sensitivity coefficient indicates that the reaction exhibits a promoting effect on ignition, while a positive coefficient inhibits the reactivity.

Figure 9 depicts the sensitivity analysis for the EG/O_2/Ar mixture at 1350 K, pressure of 5 atm and equivalence ratios of 0.5, 1.0, and 2.0 with a fuel concentration of 0.4%. The chain branching reaction H + O_2 = O + OH shows the strongest promoting effect at all equivalence ratios, since this reaction accelerates the formation of two active radicals of OH and O. The direct C−C bond dissociation reaction EG(+M) = $2CH_2OH$(+M) has high negative sensitivity coefficient, whereas the H_2O elimination reaction EG(+M) = C_2H_3OH + H_2O(+M) shows an inhibiting effect on ignition. For different equivalent ratios, the sensitivity coefficients of these main promoting reactions are close, but a significant difference is obtained for the sensitivity coefficients of the main inhibiting reactions. The strongest inhibiting reaction under stoichiometric ratio and fuel-lean conditions is HO_2 + OH = H_2O+O_2, while H_2 + O_2 = H + HO_2 turns to be the strongest inhibiting reaction under fuel-rich conditions. It is noted that H-abstraction reactions from EG by H and OH radicals to produce $CH_2OHCHOH$ radical show positive sensitivity coefficients, while H-abstraction reactions from EG oxidation intermediates, $CH_2OHCHOH$ and CH_2OHCHO species, show negative sensitivity coefficients to EG oxidation. The EG involved inhibiting reactions show a larger effect at a higher equivalence ratio, which may lead to a longer ignition delay time of EG.

https://doi.org/10.1021/acsomega.2c00275
ACS Omega 2022, 7, 9044−9052

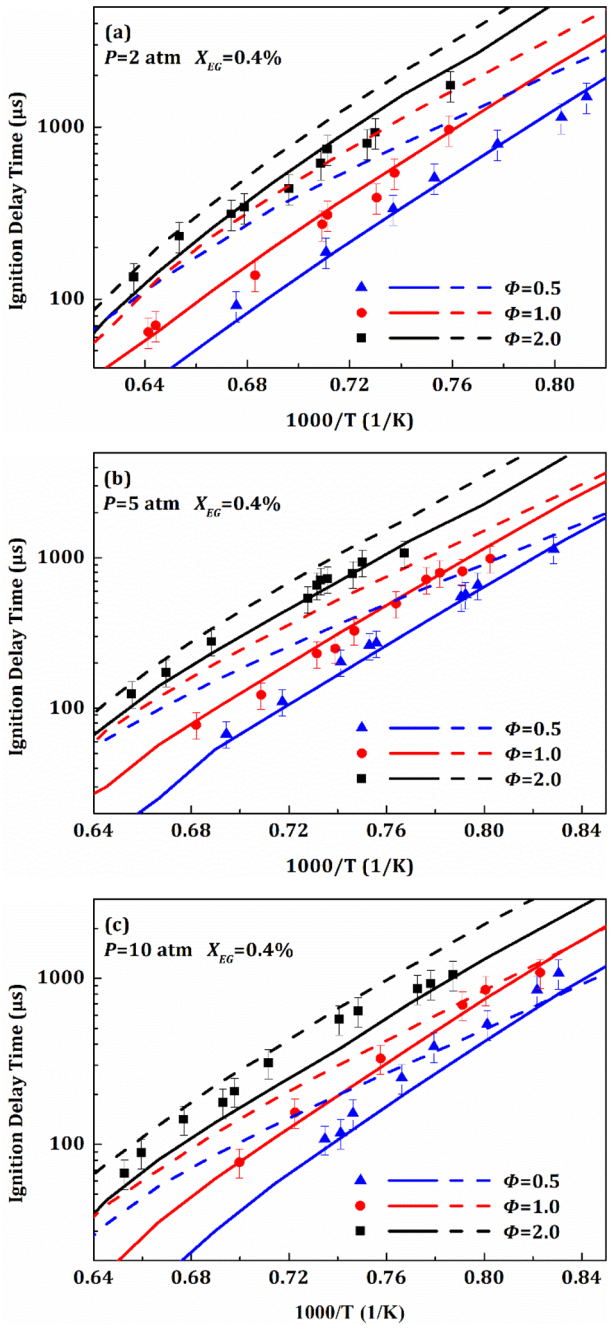

Figure 4. Effect of equivalence ratio on the ignition delay time of EG/O_2/Ar mixtures at P = 2 (a), 5 (b), and 10 atm (c) and a comparison with kinetic mechanisms. Symbols: Current experimental data. Solid line: Simulation results from the Bohon mechanism. Dashed line: Simulation results from the Kathrotia mechanism.

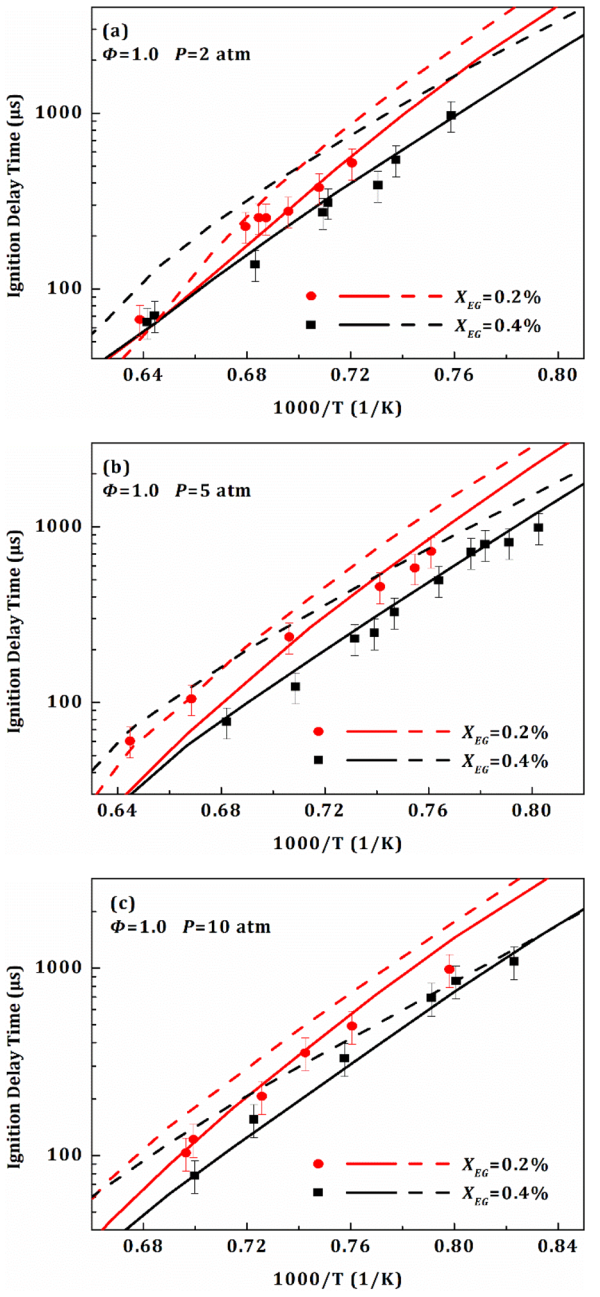

Figure 5. Effect of fuel concentration on the ignition delay time of EG/O_2/Ar mixtures at P = 2 (a), 5 (b), and 10 atm (c) and comparison with kinetic mechanisms. Symbols: Current experimental data. Solid line: Simulation results from the Bohon mechanism. Dashed line: Simulation results from the Kathrotia mechanism.

3.4. Comparison with Ethanol. Chemically, EG contains two hydroxyl groups and has a structure similar to ethanol. In current work, autoignition property of EG has been compared to ethanol. Ignition delay times of 1.5% EG/O_2/Ar mixture and 1.5% ethanol/O_2/Ar mixture were measured at approximately 2 atm and Φ = 1.0. The comparison is illustrated in Figure 10. Moreover, ignition delay times of ethanol collected at the same condition from Noorani et al.[41] were added. The results of ethanol are in good agreement with each other. The ignition delay time of ethanol is dramatically longer than that of EG, by a factor of 2.0 at high temperature of 1350 K, and the difference gradually decreases as temperature decreases. The mechanism of Bohon et al.[34] generally shows acceptable predictions of ethanol and EG ignition delay times over the test conditions.

To clarify the difference of ignition between ethanol and EG fuel at high temperature, the kinetic mechanism of Bohon et al. was used to analysis the oxidation pathway of ethanol. Figure 11 depicts the main pathway of ethanol stoichiometric mixtures ignition at 1350 K and 2 atm at 20% fuel consumption.

Similar to EG, the consumption of ethanol is also dominated by H-abstraction reactions, but the asymmetric nature of the ethanol molecule results in a greater variety of radicals created

https://doi.org/10.1021/acsomega.2c00275
ACS Omega 2022, 7, 9044−9052

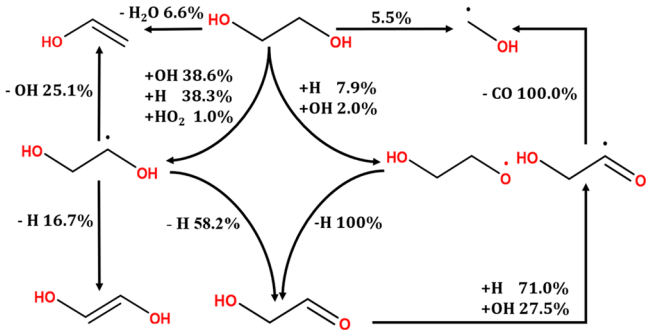

Figure 6. Reaction pathway for EG/O_2/Ar ignition at T = 1350 K, P = 5 atm, and Φ = 1.0 with 20% fuel conversion.

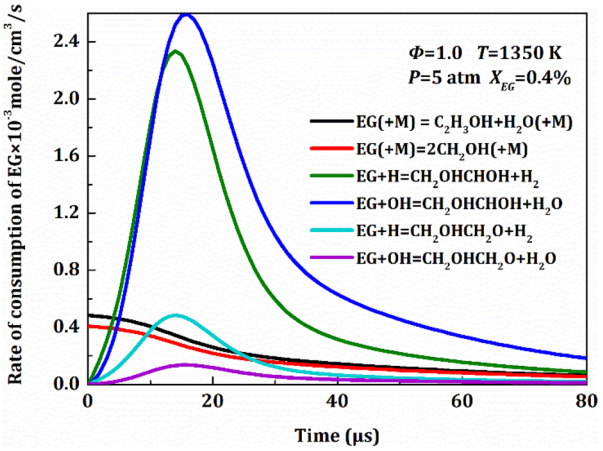

Figure 7. Rate of consumption analysis of EG at T = 1350 K, P = 5 atm, and Φ = 1.0.

through this initial reaction compared to EG. H-abstraction reactions can occur from three unique sites in ethanol oxidation. Carbons from ethanol are referred to as the α-carbon and the β-carbon, starting from the carbon attached to the OH group. The main H-abstraction reaction occurs from α-scission of the C−H bond to produce the CH_3CHOH radical, which accounted for 71.4% of ethanol consumption. CH_3CHOH can further dehydrogenate to generate acetaldehyde. The H-abstraction reaction occurring from β-scission of the C−H bond results in the CH_2CH_2OH radical, which contributes 12.8% to ethanol consumption. Both CH_3CHOH and CH_2CH_2OH radicals can further dehydrogenate to generate the ethenol molecule (C_2H_3OH). Only 2.6% ethanol is consumed by the H-abstraction reaction that occurs from the OH group to produce the ethoxy radical (CH_3CH_2O). H_2O elimination and C−C bond dissociation reactions contribute small portions to ethanol consumption. Overall, the main reaction pathways of ethanol and EG show great similarity.

The molar fraction of radicals during the oxidation process were also investigated. Figure 12 shows the time-history of fuels and H and OH radicals during the oxidation process at 2 atm and 1350 K for stoichiometric mixtures. The consumption rate of EG was obviously much faster than that of ethanol in the whole process. For the oxidation of EG, H and OH concentrations show a steep rise at the early time of about 10 μs. On the other hand, H and OH concentrations rise slowly and are much lower in the oxidation of ethanol before ignition. The early accumulation of H and OH radicals can accelerate

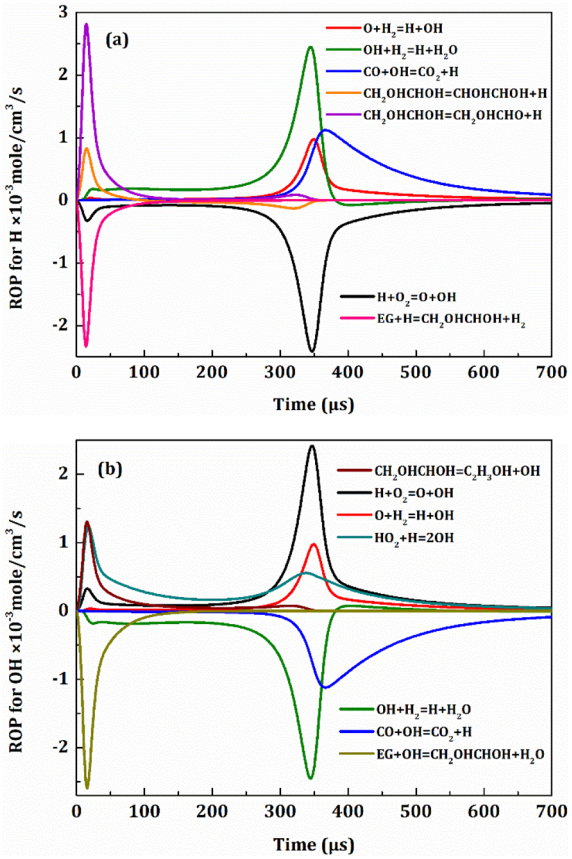

Figure 8. (a) ROP analysis of H and (b) ROP analysis of OH at T = 1350 K, P = 5 atm, and Φ = 1.0.

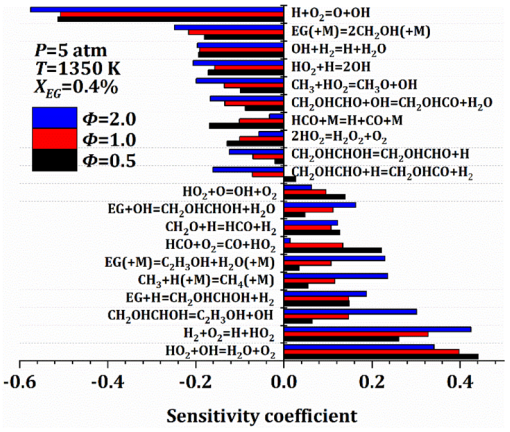

Figure 9. Sensitivity analysis for EG at T = 1350 K, P = 5 atm, X_{EG} = 0.4%, and Φ = 0.5, 1.0, and 2.0.

the ignition of EG; therefore, ignition delay times of EG are shorter than that of ethanol.

4. CONCLUSION

Autoignition characteristics of EG have been studied in a heated shock tube. Measurements of ignition delay times were carried out for gaseous EG/O_2/Ar mixtures at equivalence ratios from 0.5 to 2.0, temperatures of 1200−1600 K, and pressure of 2, 5, and 10 atm, with different fuel concentrations. Ignition delay times were determined using pressure and CH* chemiluminescence behind reflected shock waves. The effects of ignition temperature, pressure, equivalence ratio, and fuel

https://doi.org/10.1021/acsomega.2c00275
ACS Omega 2022, 7, 9044−9052

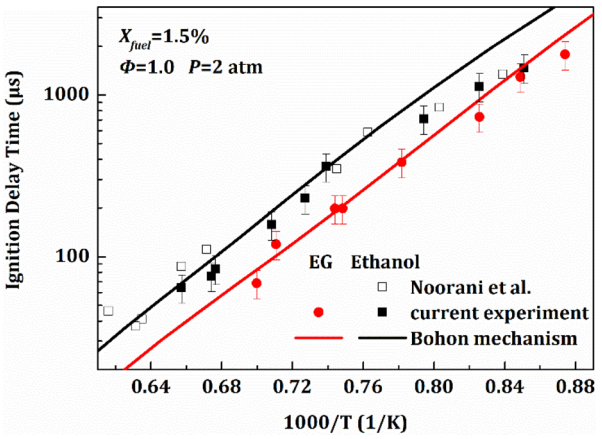

Figure 10. Comparison of ignition delay times between EG and ethanol at P = 2 atm, Φ = 1.0, and X_{fuel} = 1.5%. Symbols: experimental data. Lines: simulation results of the kinetic mechanism.

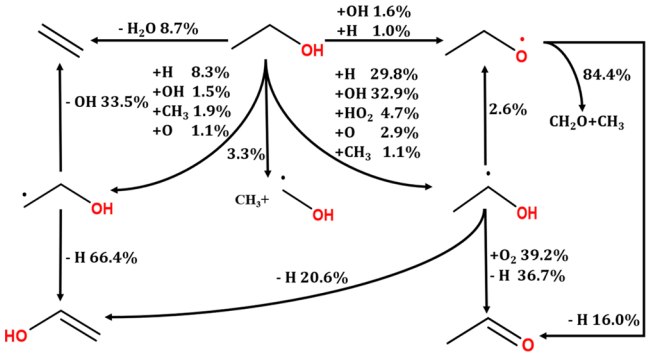

Figure 11. Reaction pathway analysis for ethanol at T = 1350 K, P = 2 atm, Φ = 1.0, and X_{fuel} = 1.5% with 20% fuel conversion.

concentration on ignition delay time were investigated. A regression analysis of the experimental data yields the following quantitative relationship:

$$\tau = (2.32 \pm 0.25) \times 10^{-5} \Phi^{(0.94\pm0.03)} P^{-(0.57\pm0.02)} X_{EG}^{-(0.33\pm0.06)} \exp[(42.02 \pm 0.73)/RT]$$

Current data have been used to evaluate the performance of two combustion mechanisms, yielding good agreement between experiments and mechanism predictions of Bohon et al. Reaction pathways analysis indicated that the consumption of EG is dominated by the H-abstraction reactions of H and OH radicals rather than the H_2O elimination or the direct C−C bond dissociation reaction. Sensitivity analysis shows that the chain branching reaction H + O_2 = O + OH shows the strongest promoting effect. H-abstraction reactions from EG have a significant inhibiting effect, while H-abstraction reactions from EG oxidation intermediates have promoting effect.

Finally, comparison between the ignition delay times of EG and ethanol has been performed. Due to the early accumulation of H and OH radicals in the oxidation of EG that is much higher and faster than that of ethanol before ignition, the ignition delay time of ethanol is dramatically longer than that of EG, by a factor of 2.0 at high temperature of 1350 K, and the difference gradually decreases as the temperature decreases.

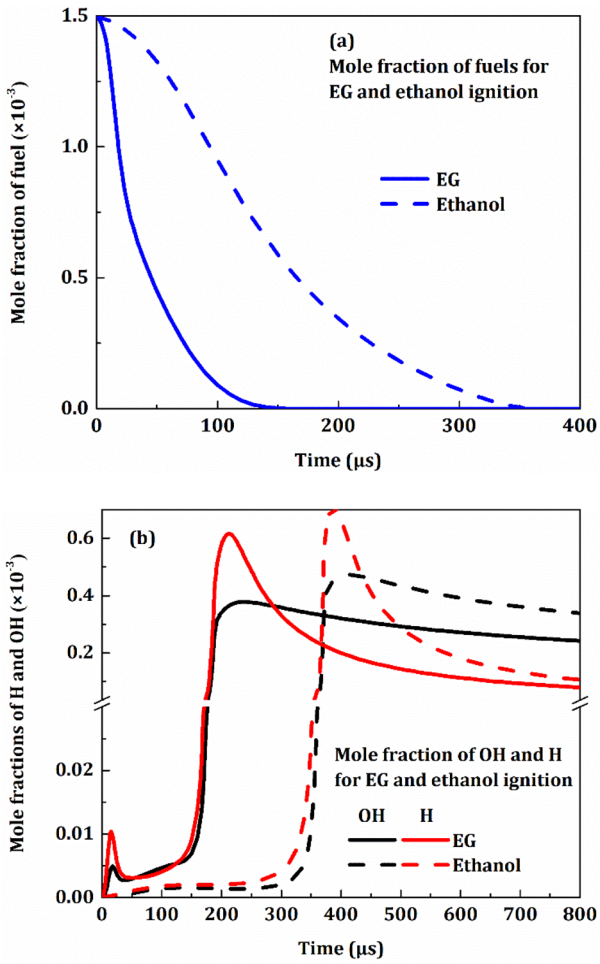

Figure 12. Mole fractions of fuels (a) and mole fractions of H and OH (b) for EG and ethanol oxidation of stoichiometric mixtures at T = 1350 K, P = 2 atm.

■ ASSOCIATED CONTENT

Supporting Information

The Supporting Information is available free of charge at https://pubs.acs.org/doi/10.1021/acsomega.2c00275.

All experimental data of ignition delay times in this work (PDF)

■ AUTHOR INFORMATION

Corresponding Author

Changhua Zhang − *Institute of Atomic and Molecular Physics, Sichuan University, Chengdu 610065, China; Engineering Research Center of Combustion and Cooling for Aerospace Power, Ministry of Education, Sichuan University, Chengdu 610065, China;* orcid.org/0000-0002-0974-3455; Email: zhangchanghua@scu.edu.cn

Authors

Ping Xu − *Institute of Atomic and Molecular Physics, Sichuan University, Chengdu 610065, China*

Rui Wang − *Institute of Atomic and Molecular Physics, Sichuan University, Chengdu 610065, China; College of Chemical Engineering, Sichuan University, Chengdu 610065, China*

Tao Ding − *Institute of Atomic and Molecular Physics, Sichuan University, Chengdu 610065, China*

https://doi.org/10.1021/acsomega.2c00275
ACS Omega 2022, 7, 9044−9052

Weixin Tang − *Institute of Atomic and Molecular Physics, Sichuan University, Chengdu 610065, China*

Complete contact information is available at: https://pubs.acs.org/10.1021/acsomega.2c00275

Notes

The authors declare no competing financial interest.

■ ACKNOWLEDGMENTS

This work is supported by the National Natural Science Foundation of China (No. 91841301).

■ REFERENCES

(1) Doppalapudi, A. T.; Azad, A. K.; Khan, M. M. K. Combustion chamber modifications to improve diesel engine performance and reduce emissions: A review. *Renew. Sustain. Energy Rev.* **2021**, *152*, 111683.

(2) Khalife, E.; Tabatabaei, M.; Demirbas, A.; Aghbashlo, M. Impacts of additives on performance and emission characteristics of diesel engines during steady state operation. *Prog. Energy Combust. Sci.* **2017**, *59*, 32−78.

(3) Hoang, A. T.; Le, A. T.; Pham, V. V. A core correlation of spray characteristics, deposit formation, and combustion of a high-speed diesel engine fueled with Jatropha oil and diesel fuel. *Fuel.* **2019**, *244*, 159−175.

(4) Hazar, H.; Sevinc, H.; Sap, S. Performance and emission properties of preheated and blended fennel vegetable oil in a coated diesel engine. *Fuel.* **2019**, *254*, 115677.

(5) Mohd Noor, C. W.; Noor, M. M.; Mamat, R. Biodiesel as alternative fuel for marine diesel engine applications: A review. *Renew. Sustain. Energy Rev.* **2018**, *94*, 127−142.

(6) Mirhashemi, F. S.; Sadrnia, H. NOx emissions of compression ignition engines fueled with various biodiesel blends: A review. *J. Energy Inst.* **2020**, *93*, 129−151.

(7) Masera, K.; Hossain, A. K. Biofuels and thermal barrier: A review on compression ignition engine performance, combustion and exhaust gas emission. *J. Energy Inst.* **2019**, *92*, 783−801.

(8) Dabi, M.; Saha, U. K. Application potential of vegetable oils as alternative to diesel fuels incompression ignition engines: A review. *J. Energy Inst.* **2019**, *92*, 1710−1726.

(9) Ghadikolaei, M. A.; Wong, P. K.; Cheung, C. S.; Ning, Z.; Yung, K.-F.; Zhao, J.; Gali, N. K.; Berenjestanaki, A. V. Impact of lower and higher alcohols on the physicochemical properties of particulate matter from diesel engines: A review. *Renew. Sustain. Energy Rev.* **2021**, *143*, 110970.

(10) Mahmudul, H. M.; Hagos, F. Y.; Mamat, R.; Adam, A. A.; Ishak, W. F. W.; Alenezi, R. Production, characterization and performance of biodiesel as an alternative fuel in diesel engines − A review. *Renew. Sustain. Energy Rev.* **2017**, *72*, 497−509.

(11) Kalil Rahiman, M.; Santhoshkumar, S.; Subramaniam, D.; Avinash, A.; Pugazhendhi, A. Effects of oxygenated fuel pertaining to fuel analysis on diesel engine combustion and emission characteristics. *Energy.* **2022**, *239*, 122373.

(12) Zhu, Q.; Zong, Y.; Yu, W.; Yang, W.; Kraft, M. Understanding the blending effect of polyoxymethylene dimethyl ethers as additive in a common-rail diesel engine. *Appl. Energy.* **2021**, *300*, 117380.

(13) Çelebi, Y.; Aydın, H. An overview on the light alcohol fuels in diesel engines. *Fuel.* **2019**, *236*, 890−911.

(14) Yesilyurt, M. K.; Cakmak, A. An extensive investigation of utilization of a C8 type long-chain alcohol as a sustainable next-generation biofuel and diesel fuel blends in a CI engine − The effects of alcohol infusion ratio on the performance, exhaust emissions, and combustion characteristics. *Fuel* **2021**, *305*, 121453.

(15) Nour, M.; Attia, A. M. A.; Nada, S. A. Combustion, performance and emission analysis of diesel engine fuelled by higher alcohols (butanol, octanol and heptanol)/diesel blends. *Energy Convers. Manage.* **2019**, *185*, 313−329.

(16) Atmanli, A.; Yilmaz, N. An experimental assessment on semi-low temperature combustion using waste oil biodiesel/C3-C5 alcohol blends in a diesel engine. *Fuel.* **2020**, *260*, 116357.

(17) Campos-Fernández, J.; Arnal, J. M.; Gómez, J.; Dorado, M. P. A comparison of performance of higher alcohols/diesel fuel blends in a diesel engine. *Appl. Energy.* **2012**, *95*, 267−275.

(18) Kumar, S.; Cho, J. H.; Park, J.; Moon, Il. Advances in diesel−alcohol blends and their effects on the performance and emissions of diesel engines. *Renew. Sustain. Energy Rev.* **2013**, *22*, 46−72.

(19) Rajesh Kumar, B.; Saravanan, S. Use of higher alcohol biofuels in diesel engines: A review. *Renew. Sustain. Energy Rev.* **2016**, *60*, 84−115.

(20) Wu, S.; Kang, D.; Liu, Y.; Wang, Z.; Xiao, R.; Boehman, A. L. The oxidation of C2-C4 diols and diol/TPGME blends in a motored engine. *Fuel.* **2019**, *257*, 116093.

(21) Wu, S.; Yang, H.; Hu, J.; Shen, D.; Zhang, H.; Xiao, R. The miscibility of hydrogenated bio-oil with diesel and its applicability test in diesel engine: A surrogate (ethylene glycol) study. *Fuel. Process. Technol.* **2017**, *161*, 162−168.

(22) Zhang, P.; He, J.; Chen, H.; Zhao, X.; Geng, L. Improved combustion and emission characteristics of ethylene glycol/diesel dual-fuel engine by port injection timing and direct injection timing. *Fuel. Process. Technol.* **2020**, *199*, 106289.

(23) Chen, H.; Zhang, P.; Liu, Y. Investigation on combustion and emission performance of a common rail diesel engine fueled with diesel-ethylene glycol dual fuel. *Appl. Therm. Eng.* **2018**, *142*, 43−55.

(24) Yalavarthi, S.; Chintalapudi, A. K.; Dev, S. Performance and emission analysis of diesel engine using oxygenated compounds. *Int. J. Adv. Sci. Technol.* **2013**, *61*, 9−16.

(25) Fradet, Q.; Braun-Unkhoff, M.; Riedel, U. A sectional approach for the entrained-flow gasification of slurry fuels. *Energy Fuels.* **2018**, *32*, 12532−12544.

(26) Fleck, S.; Santo, U.; Hotz, C.; Jakobs, T.; Eckel, G.; Mancini, M.; Weber, R.; Kolb, T. Entrained flow gasification Part 1: Gasification of glycol in an atmospheric-pressure experimental rig. *Fuel.* **2018**, *217*, 306−319.

(27) Mancini, M.; Alberti, M.; Dammann, M.; Santo, U.; Eckel, G.; Kolb, T.; Weber, R. Entrained flow gasification. Part 2: Mathematical modeling of the gasifier using RANS method. *Fuel.* **2018**, *225*, 596−611.

(28) Eckel, G.; Le Clercq, P.; Kathrotia, T.; Saenger, A.; Fleck, S.; Mancini, M.; Kolb, T.; Aigner, M. Entrained flow gasification. Part 3: Insight into the injector near-field by Large Eddy Simulation with detailed chemistry. *Fuel.* **2018**, *223*, 164−178.

(29) Ye, L.; Zhao, L.; Zhang, L.; Qi, F. Theoretical studies on the unimolecular decomposition of ethylene glycol. *J. Phys. Chem. A* **2012**, *116*, 55−63.

(30) Li, Q.; Yao, L.; Lin, S. H. Calculation of anharmonic effect on the dissociation of ethylene glycol. *J. Theor. Comput. Chem.* **2017**, *16*, 1750077.

(31) Hafner, S.; Rashidi, A.; Baldea, G.; Riedel, U. A detailed chemical kinetic model of high-temperature ethylene glycol gasification. *Combust. Theor. Model.* **2011**, *15*, 517−535.

(32) Kathrotia, T.; Naumann, C.; Oßwald, P.; Köhler, M.; Riedel, U. Kinetics of Ethylene Glycol: The first validated reaction scheme and first measurements of ignition delay times and speciation data. *Combust. Flame* **2017**, *179*, 172−184.

(33) Fernando, N.; Braun-Unkhoff, M.; Riedel, U. Modeling study of the entrained flow gasification of ethylene glycol, a surrogate fuel for a pyrolysis oil. *Energy Fuels.* **2019**, *33*, 9818−9827.

(34) Bohon, M. D.; Al Rashidi, M. J.; Sarathy, S. M.; Roberts, W. L. Experiments and simulations of NOx formation in the combustion of hydroxylated fuels. *Combust. Flame* **2015**, *162*, 2322−2336.

(35) He, J.; Gou, Y.; Lu, P.; Zhang, C.; Li, P.; Li, X. Shock tube measurements and kinetic modeling study on autoignition characteristics of cyclohexanone. *Combust. Flame* **2018**, *192*, 358−368.

(36) Shi, L.; Chen, D.; Zheng, Z.; Xu, P.; Wang, R.; Zhang, C. An experimental and kinetic study the effect of nitrogen dioxide addition on autoignition of n-heptane. *Combust. Flame* **2021**, *232*, 111540.

(37) Yang, M.; Wan, Z.; Tan, N.; Zhang, C.; Wang, J.; Li, X. An experimental and modeling study of ethylene−air combustion over a wide temperature range. *Combust. Flame* **2020**, *221*, 20−40.
(38) *ANSYS chemkin 17.0 (15151)*, ANSYS Reaction Design: San Diego, CA, 2016.
(39) Davidson, D. F.; Zhu, Y.; Shao, J.; Hanson, R. K. Ignition delay time correlations for distillate fuels. *Fuel.* **2017**, *187*, 26−32.
(40) Johnson, M. V.; Goldsborough, S. S.; Serinyel, Z.; O'Toole, P.; Larkin, E.; O'Malley, G.; Curran, H. J. A Shock tube study of n- and iso-propanol ignition. *Energy Fuels.* **2009**, *23*, 5886−5898.
(41) Noorani, K. E.; Akih-Kumgeh, B.; Bergthorson, J. M. Comparative high temperature shock tube ignition of C1-C4 primary alcohols. *Energy Fuels.* **2010**, *24*, 5834−5843.

https://doi.org/10.1021/acsomega.2c00275
ACS Omega 2022, 7, 9044−9052